

Article

Heat of Decomposition and Fire Retardant Behavior of Polyimide-Graphene Nanocomposites

Caroline J. Akinyi  and Jude O. Iroh * 

Materials Science and Engineering Program, Department of Mechanical and Materials Engineering, University of Cincinnati, Cincinnati, OH 45221, USA; akinyicj@mail.uc.edu

* Correspondence: irohj@ucmail.uc.edu

Abstract: Polyimide is a high-performance engineering polymer with outstanding thermomechanical properties. Because of its inherent fire-retardant properties, polyimide nanocomposite is an excellent material for packaging electronic devices, and it is an attractive electrode material for batteries and supercapacitors. The fire-retardant behavior of polyimide can be remarkably improved when polyimide is reinforced with multilayered graphene sheets. Differential scanning calorimetry and thermogravimetric analysis were used to study the heat of decomposition and gravimetric decomposition rate, respectively, of polyimide-graphene nanocomposites. Polyimide/graphene nanocomposites containing 10, 20, 30, 40, and 50 wt.% of multilayered graphene sheets were heated at a rate of 10 and 30 °C/min in air and in nitrogen atmosphere, respectively. The rate of mass loss was found to remarkably decrease by up to 198% for nanocomposites containing 50 wt.% of graphene. The enthalpy change resulting from the decomposition of the imide ring was found to decrease by 1166% in nitrogen atmosphere, indicating the outstanding heat-shielding properties of multilayered graphene sheets due to their high thermal conductivity. Graphene sheets are believed to form a continuous carbonaceous char layer that protects the imide ring against decomposition, hence decreasing initial mass loss. The enthalpy changes due to combustion, obtained from differential scanning calorimetry, were used to calculate the theoretical heat release rates, a major parameter in the determination of flammability of polymers. The heat release rate decreased by 62% for composites containing 10 wt.% of graphene compared to the neat polyimide matrix. Polyimide has a relatively lower heat of combustion as compared with graphene. However, graphene significantly decreases the mass loss rates of polyimide. The combined interaction of graphene and polyimide led to an overall decrease in the heat release rate. It is noted that both mass loss rate and heat of combustion are important factors that contribute to the rate of heat released.



Citation: Akinyi, C.J.; Iroh, J.O. Heat of Decomposition and Fire Retardant Behavior of Polyimide-Graphene Nanocomposites. *Energies* **2021**, *14*, 3948. <https://doi.org/10.3390/en14133948>

Academic Editor: Prodip K. Das

Received: 25 May 2021

Accepted: 24 June 2021

Published: 1 July 2021

Publisher's Note: MDPI stays neutral with regard to jurisdictional claims in published maps and institutional affiliations.



Copyright: © 2021 by the authors. Licensee MDPI, Basel, Switzerland. This article is an open access article distributed under the terms and conditions of the Creative Commons Attribution (CC BY) license (<https://creativecommons.org/licenses/by/4.0/>).

Keywords: nanocomposites; polyimide; graphene nanosheets; flame-retardant; differential scanning calorimetry; thermogravimetry

1. Introduction

Polymer nanocomposites are a class of flame retardant technology that was discovered in the early 1990s and has been shown to result in dramatic decreases in peak heat release rates [1,2]. Nanocomposites also enhance other properties of the final system, such as mechanical properties, unlike most flame retardants that are known to decrease the mechanical properties. However, nanocomposites have to be used in combination with other flame retardants in order to meet flame retardancy regulatory requirements [3]. Nanocomposites enhance flame retardancy by forming a barrier around the underlying polymer, which slows down the mass degradation and heat release rates [4–7]. Polymers containing graphene and layered silicates have been the focus of extensive research [8–10]. Even at low loadings (<20 wt.%), these nanofillers significantly change the properties of the materials [11,12].

Graphene, a one atom thick, two-dimensional sheet of sp² bonded carbon atoms arranged in a honeycomb structure, has generated great interest amongst material scientists

because of its exceptional intrinsic properties [13]. Single-layered graphene has been reported to have Young's modulus of 1 TPa and ultimate strength of up to 130 GPa [14]. Thermal conductivity of 5000 W/(mK) [15] and electrical conductivity of 6000 s/cm [16] have been reported. It also has an extremely high surface area and has permeability [17]. When used in the fabrication of polymer nanocomposites, it results in the improvement of mechanical, electrical, thermal, and gas barrier properties of the polymers.

Aromatic polyimide is a high-performance thermosetting polymer with excellent thermal and thermooxidative stability, radiation and chemical resistance, and mechanical properties. Fiber-reinforced polyimide composites have found applications in the aerospace industries where they are used to replace metal counterparts, resulting in fuel savings due to reduced weight. It is also used to avoid corrosion issues often encountered by metals or ceramics. However, their use as replacement parts for metals or ceramics means that they have to withstand extreme operation temperatures [18]. Polyimide still suffers from thermal oxidative degradation that slowly wears off the materials, resulting in structural failure of the composites [19–22]. The addition of nanofillers, such as graphene, to organic polymers has resulted in the improvement of thermal stability because of the mass transport barrier to volatiles generated during thermal decomposition and thermal isolation effect of sheets [23,24].

The pyrolytic degradation of an organic polymer in the condensed phase to yield combustible volatile products can be regarded as the first stage in the flaming combustion of the polymer. The presence of flame retardants in the polymer can affect the rate and mode of pyrolysis of the polymer in the condensed phase [25]. The use of DSC and TGA techniques can provide insight into the stages of pyrolytic breakdown of polymers, their thermal stability, and the nature and amount of solid residues and volatile products [25]. The role played in combustion by the initial condensed phase burning of the polymer can, therefore, be well understood from these studies.

Direct measurement of the flammability and fire behavior of materials requires large quantities of materials and can be prohibitively expensive. In this work, the thermal stability and combustion properties of milligram-sized samples were obtained using differential scanning calorimetry (DSC) and thermogravimetric analysis (TGA).

2. Materials and Methods

Graphene powder with the characteristics listed in Table 1 was purchased from Global Graphene Group, Dayton, OH, USA.

Table 1. Characteristics of graphene powder.

Average Lateral Dimension (mm)	Thickness (nm)	Oxygen Content (%)	Specific Surface Area m ² /g	Density (g/cm ³)	Carbon (wt.%)	Hydrogen (wt.%)	Nitrogen (wt.%)	Oxygen (wt.%)
7	70–100	<1	10–15	0.1–0.3	≥97	≤1	≤0.5	≤2

As shown in Table 1, the graphene used is not single-layer and is relatively cheaper in terms of production cost than the single-layer graphene. The samples fabricated used up to 50 wt.% graphene powder, while maintaining good dispersibility within the polymer matrix with no need for chemical functionalization.

Pyromellitic dianhydride (99% purity), 4,4-oxydianiline and N-methyl-pyrrolidone (99% purity), were purchased from Sigma-Aldrich.

2.1. Synthesis of Graphene/Polyamic Acid

5.2 g of 4,4-oxydianiline (ODA) was added to 100 mL of N-methyl-pyrrolidone (NMP) contained in a round-bottomed flask followed by mechanical stirring until the solid completely dissolved in the solvent. Graphene quantity corresponding to 10 wt.% of total solids was added to the solution and stirring continued for 8 h. Pyromellitic dianhydride

(PMDA) was then added to the mixture, followed by stirring for 12 h, the temperature was maintained at 10 °C. Subsequent mixtures containing 20, 30, 40, and 50 wt.% graphene were synthesized.

2.2. Fabrication of Graphene-Polyimide Films

The mixture was solution casted on a glass substrate followed by thermal imidization in a vacuum oven at 120 °C for 2 h and 200 °C for 1 h to form polyimide-graphene composite films (PI-NGS).

2.3. Thermal Analysis

The films were subjected to heating rates of 10 °C/min from 25 °C to 725 °C in nitrogen and air atmospheres in a DSC Q20 thermal analyzer purchased from TA instruments, New Castle, Delaware, USA. In TGA, the films were heated from 25 °C to 1000 °C in nitrogen and air at a heating rate of 30 °C/min in a TGA Q50 Thermal Analyzer purchased from TA Instruments, New Castle, DE, USA.

3. Results and Discussion

Figure 1 shows the TGA weight loss curves of neat polyimide obtained at 30 °C/min in air and in nitrogen. Degradation of polyimide in nitrogen occurs in a single step resulting in the formation of approximately 60% char, as has also been reported by Lua et al. [26]. Reaction mechanism proposed by Hatori et al. [27] and also reported by Cella [28] indicates that the imide ring is the site of initial degradation. This is evidenced by the production of carbon monoxide in large quantities. The cleavage of the imide ring leads to the formation of isocyanate groups as intermediates, with the release of carbon monoxide. With further heat treatment, the isocyanate groups combine, leading to the release of carbon dioxide. Other fragments in the residue combine to form aromatic and heteroaromatic rings, with hydrogen released as a by-product. Volatile by-products detected by various groups are: Phenol, aniline, cyanobenzene, dicyanobenzenes, and phthalimide, in addition to CO, CO₂, H₂, and N₂.

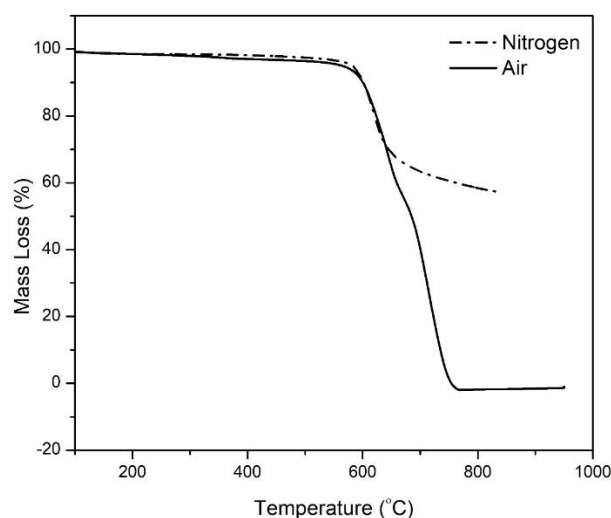


Figure 1. Thermogravimetric mass loss profiles of neat polyimide in air and nitrogen.

Burger et al. [29] concluded that the residual char comprised mostly planar polyaromatics. Their proposed degradation mechanism is shown in Figure 2. Evolved gas analysis was used to predict the degradation mechanism.

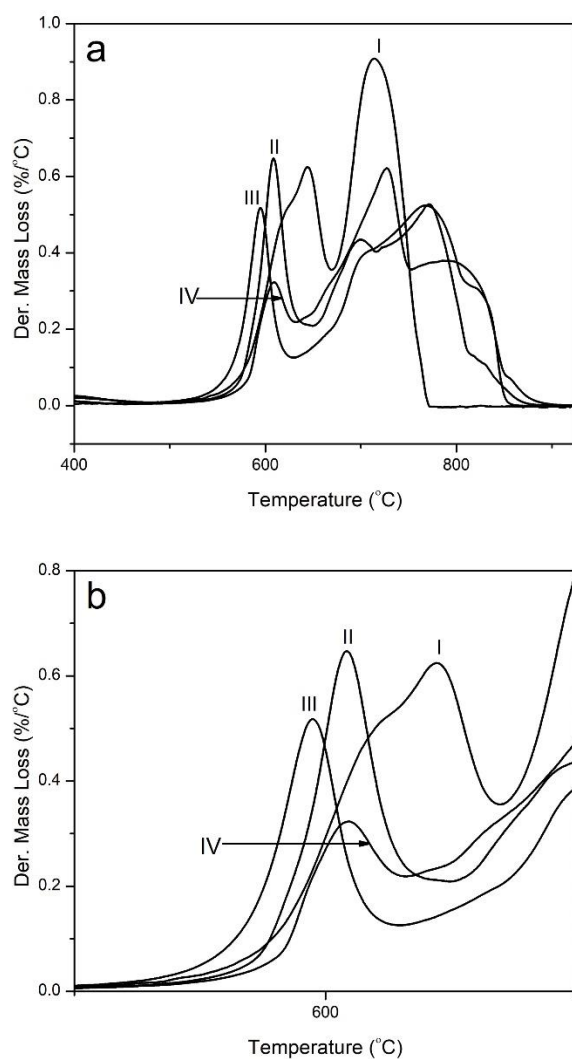


Figure 3. Derivative mass loss curves: (a) for (I) Neat PI, (II) PI-10 wt.% graphene, (III) PI-30 wt.% graphene, (IV) PI-50 wt.% graphene; (b) for imide ring decomposition for neat PI (I) and the composites (II–IV).

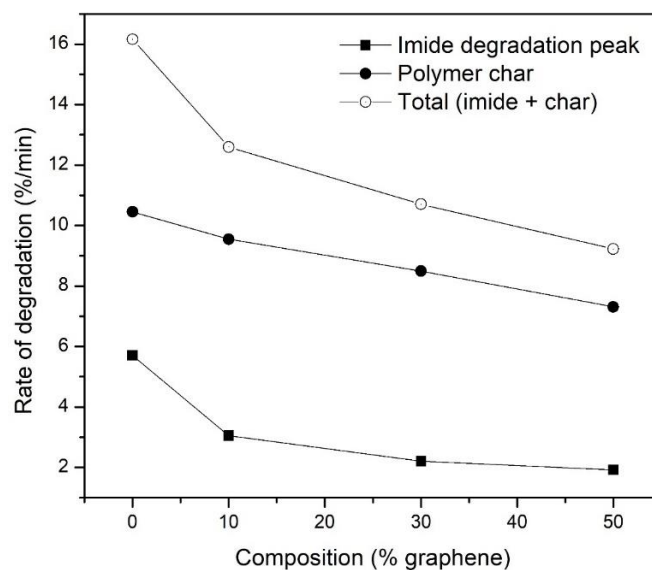


Figure 4. Rate of degradation of imide peak and polyimide char of neat PI and PINGS composites.

The rate of degradation of the polymer char is also shown to decrease in the presence of graphene. From SEM and EDX analysis, it was ascertained that graphene does not undergo appreciable degradation in inert atmosphere. It, therefore, densifies and fortifies the polymer char, hence, decreasing its propensity to degrade.

The SEM images in Figure 5 show that the char structure of neat polyimide and the composites degraded in nitrogen atmosphere to a temperature of 900 °C. The neat polymer char shows a highly porous morphology, however, for composites with increasing graphene content, the porosity significantly decreases and completely disappears, forming a strong dense char layer. The formation of a dense char layer and reduction in porosity inhibits the evolution of volatile components and slows down polyimide degradation.

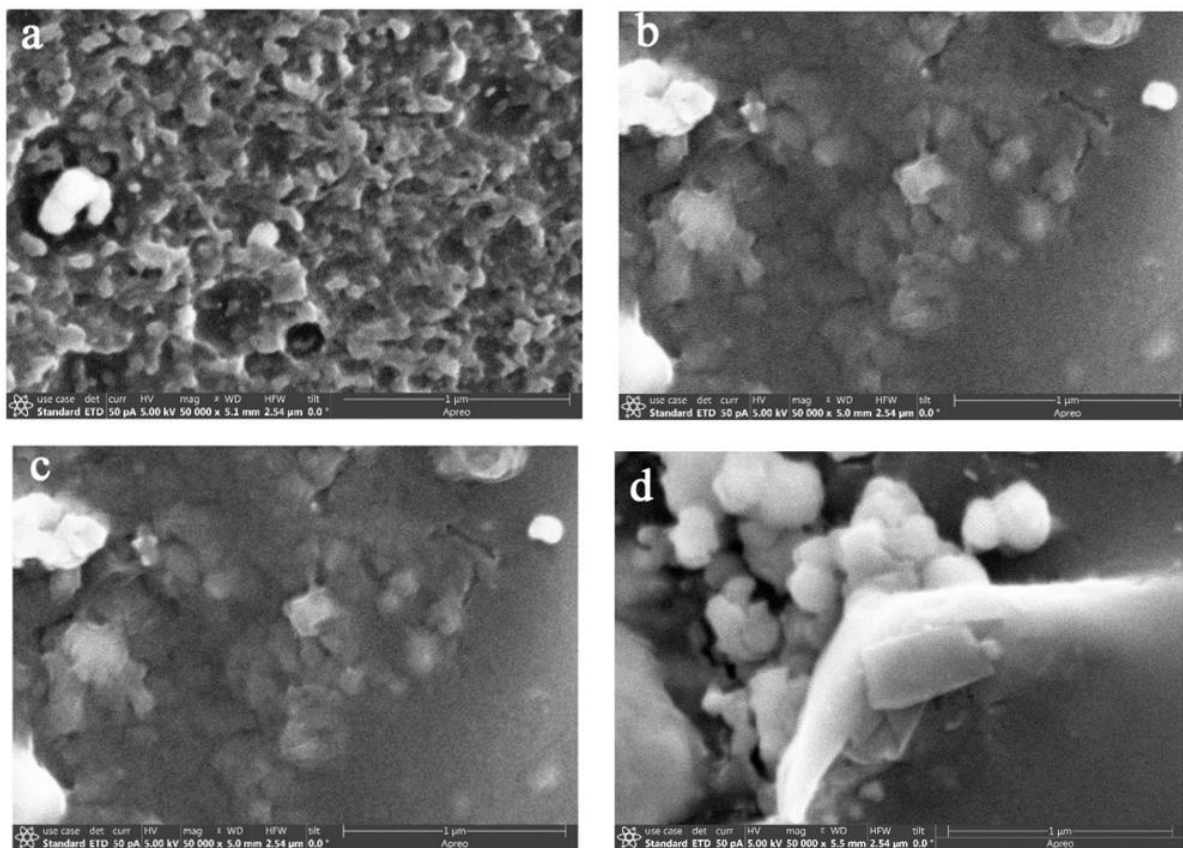


Figure 5. SEM images of the char residues at 900 °C for: (a) Neat PI; (b) PI-10 wt.% NGS; (c) PI-30 wt.% NGS; (d) PI-50 wt.% NGS at 50,000 \times .

Table 2 presents the summary of EDX area analyses from selected areas of the SEM images for the char residue. Based on the molecular weight of one repeat unit of polyimide, the percentage of carbon, nitrogen and oxygen in the non-degraded polymer is 70.97%, 7.53%, and 21.5%, respectively. The EDX analysis of neat polyimide char shows that the carbon percentage increased by 26% to 98.2%, while the oxygen percentage decreased by 20% to 1.8%. Following the degradation mechanism proposed in Figure 2, the planar polyaromatics structures in the char are expected to comprise mainly of carbon with negligible quantities of oxygen, nitrogen, and hydrogen. The fact that hydrogen and nitrogen are not observed in the EDX analysis of the neat PI char may indicate that their quantities are below the lower limit of detection of the instrument.

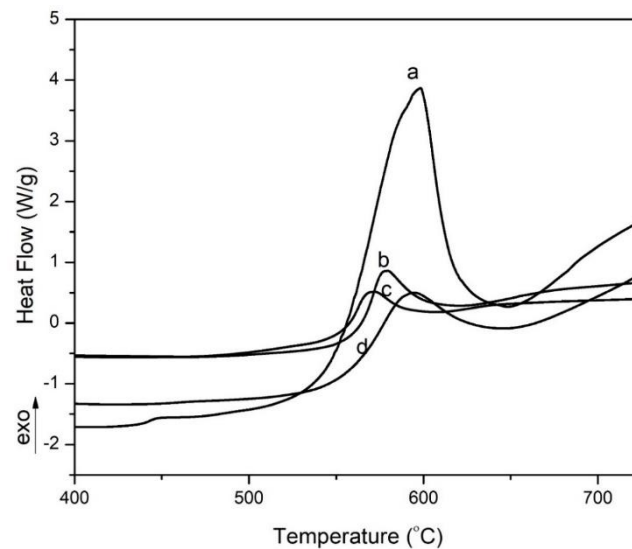
Table 2. SEM-EDX analysis of char from neat polyimide, grapheme, and composites containing 10, 30, and 50 wt.% graphene.

Sample	Carbon (%)	Oxygen (%)	Nitrogen (%)	Silicon (%)
Neat PI	98.2	1.8	-	-
PI-10	96.2	1.6	2.2	-
PI-30	96.7	1.5	1.9	-
PI-50	96.7	1.1	1.6	0.7
Graphene	96.7	2.3	0.3	0.7

The composites containing graphene show some detectable levels of nitrogen, indicating that there is some protection of the polymer char from the extensive degradation observed in the neat polymer. This explains the higher levels of nitrogen-containing groups in the composite. The composite containing 10 wt.% graphene has a higher percentage of nitrogen compared to the composites with higher loadings of graphene. This indicates better protection of the polymer char at lower loadings, which can be attributed to better dispersion of the graphene in the polymer matrix at lower loadings.

The planar polyaromatic structures formed as residue in the initial degradation stage undergo complete degradation at the second stage in air atmosphere, followed by the degradation of the more crystalline and highly graphitized graphene char at higher temperatures (Figure 3a).

DSC thermograms (Figure 6) show the heat flow during the degradation of the samples in nitrogen. This is the heat released because of cleavage of the imide ring followed by recombination reactions of the intermediate products leading to a stable char comprised of planar polyaromatics.

**Figure 6.** DSC thermograms obtained in nitrogen: (a) neat polyimide; (b) PI-30 wt.% grapheme; (c) PI-50 wt.% grapheme; (d) PI-10 wt.% grapheme.

Total enthalpy change for the degradation process was obtained by numeric integration of the DSC peak over the temperature interval and expressed in kJ/g. At constant pressure, the heat capacity equals the change in enthalpy, as expressed in Equation (1) [32].

$$C_p = \left(\frac{\partial H}{\partial T} \right)_p \quad (1)$$

The total enthalpy change over the temperature range (T_1, T_2) is given by Equation (2).

$$\Delta H = \int_{T_1}^{T_2} \left(\frac{\partial H}{\partial T} \right)_p dT = \int_{T_1}^{T_2} C_p dT \quad (2)$$

PI-NGS composites release significantly less heat upon degradation than the neat polymer, a 1100% decrease is observed between the neat PI and the composite containing 50 wt.% graphene. The trend is shown in Figure 7. This trend suggests that graphene acts by shielding the imide ring, leading to a decreased extent of degradation of the matrix, hence, preserving its structural integrity. The retention of substantial amounts of carbonaceous protective layer due to the presence of graphene leads to lower rates of heat transfer and significantly less mass loss of polymers [33,34].

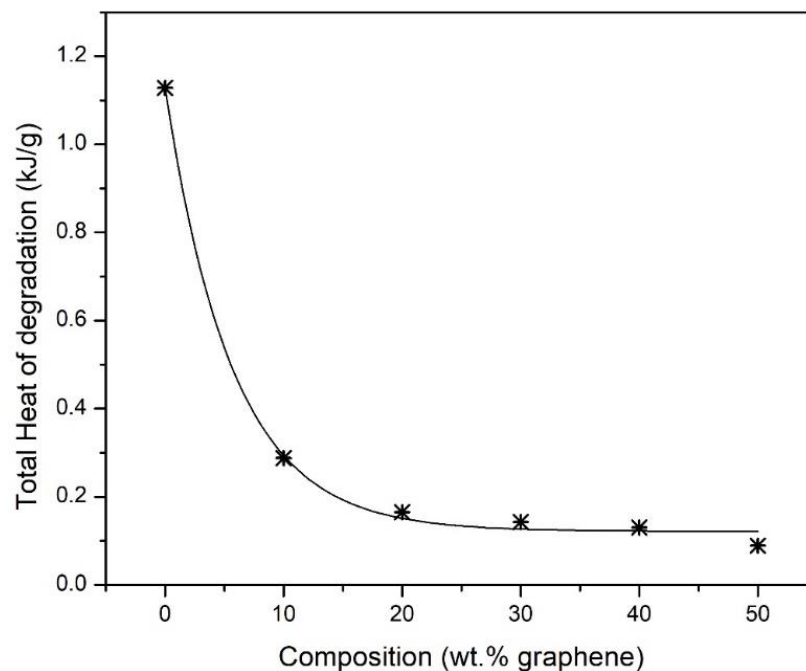


Figure 7. Total heat released during the degradation of PI and PINGS composites in nitrogen at a heating rate of 10 °C/min.

DSC thermograms in air, shown in Figure 8, show two distinct peaks for the neat PI and slightly broadened and staggered peaks for the PI-NGS composites. Multiple peaks indicate that the mechanism of degradation in air is different from that in inert atmosphere. The intermediates formed from the cleavage of the imide ring react with oxygen to form an oxidized product that is more stable and requires higher activation energy for its decomposition, hence, it decomposes at higher temperatures. Pramoda et al. [35] did a kinetic study of the degradation of polyimide in air and in nitrogen atmospheres. They reported that the activation energies were stable in nitrogen and air for the initial weight loss. However, there was a jump at 40% weight loss in air, which they postulated was due to the formation of a more stable oxidation product that required higher activation energy for its decomposition.

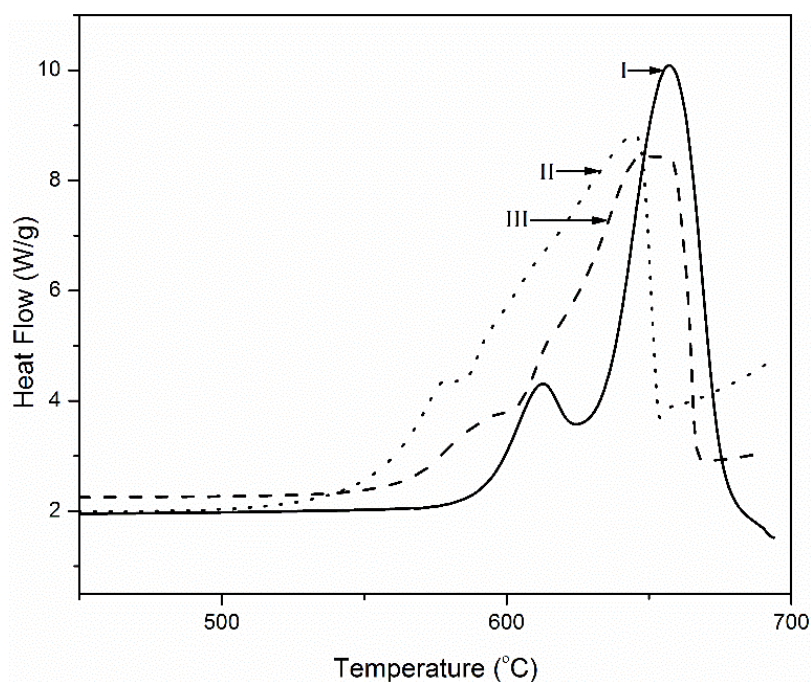


Figure 8. DSC thermograms obtained in air (I) Neat polyimide, (II) Polyimide-50 wt.% grapheme, (III) Polyimide-30 wt.% grapheme ($\beta = 10\text{ }^{\circ}\text{C}/\text{min}$).

Onset degradation temperature is a measure of ignitibility of a sample. Fuel consumption and volatiles generation begin at this temperature. This is determined in DSC by the first detected deviation from the baseline. Graphene is shown to have little to no effect on the ignitibility of the polymer. This is reflected in the nearly constant onset of degradation temperature both in air and in nitrogen atmospheres. The imide bond, which is the site for initial degradation, has a lower bond enthalpy (average bond enthalpy = 293 kJ/mol), and therefore, easily degrades at elevated temperatures.

Enthalpy change due to degradation of the imide ring in nitrogen was compared to that in air, as shown in Figure 9. There is a 70% decrease in the heat of degradation of the imide ring in nitrogen compared to that in air. This might be due to the formation of more stable oxidation products that protect the imide bond from further degradation. The heat of degradation of the PI-NGS composites is slightly higher in air than in nitrogen, but constant across the different compositions, as is observed in nitrogen atmosphere too. Polymer degradation occurs faster in air or oxygen than in an inert atmosphere. Reactions between oxygen and alkoxy radicals (RO^{\bullet}) released from initial degradation products accelerate the degradation of the polymer matrix. This leads to an increased concentration of polymer alkyl radicals (R^{\bullet}) that lead to high levels of scission and cross-linked products. [36].

Mass loss rates obtained from TGA measurements and enthalpy changes calculated from DSC thermograms were used to estimate the theoretical heat release rates. With the knowledge of the enthalpy changes due to degradation in air, the theoretical heat release rate is calculated by:

$$\dot{q} = \Delta H \times \dot{m}_{fuel} \quad (3)$$

where ΔH is the enthalpy change due to combustion and \dot{m}_{fuel} is the mass loss rate [37]. The uncertainty analysis of this method leads to an error of <10%, assuming complete combustion. This method has few parameters, hence, less propagation of errors.

From Equation (3), the theoretical heat release rates of neat polyimide, grapheme, and polyimide-graphene composites were obtained and graphed in Figure 10. The trend shows that the heat release rate decreases by 62% at 10 wt.% grapheme.

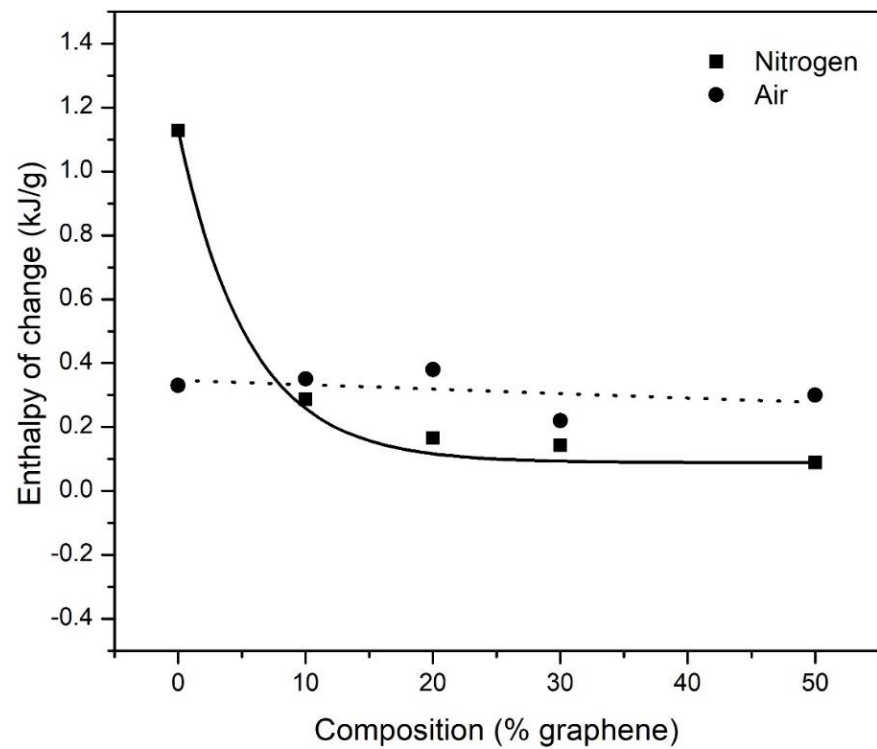


Figure 9. Enthalpy changes of neat PI and PI-NGS composites due to the degradation of the imide bond as measured by DSC in nitrogen and air at a heating rate of 10 °C/min.

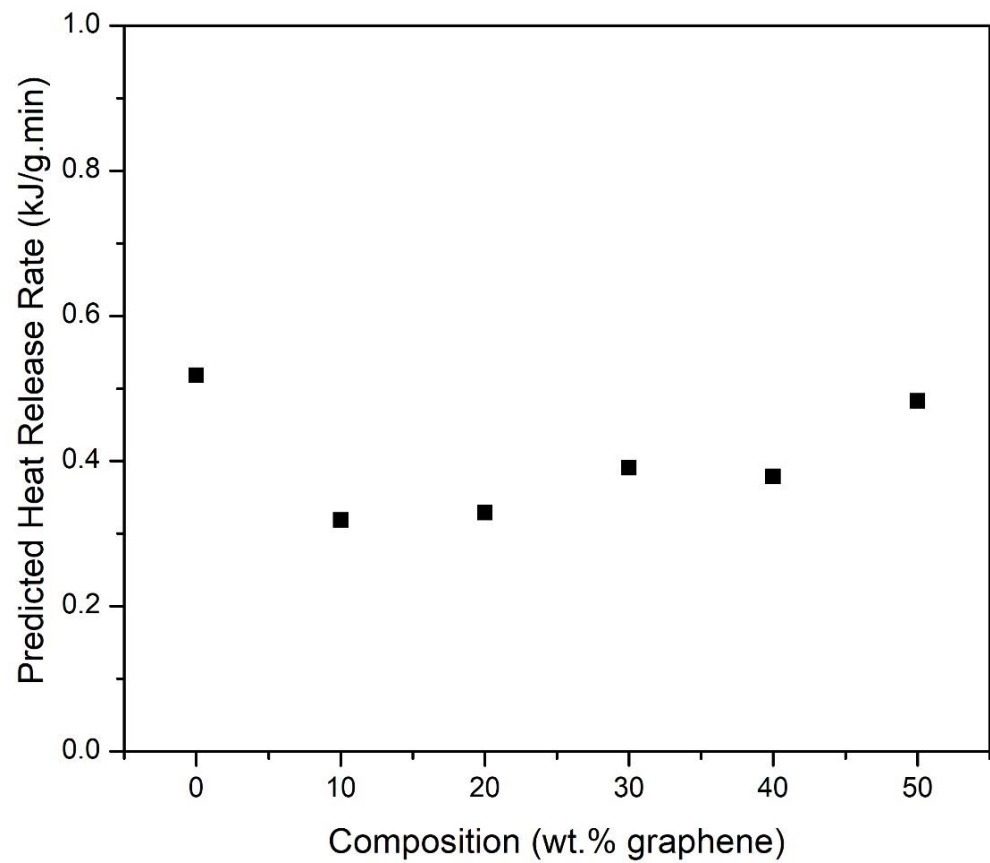


Figure 10. Predicted heat release rates as a function of wt.% graphene.

The enthalpy change due to the combustion of graphene is reportedly higher than that of neat polyimide [38,39]. Both graphene and polyimide contribute to the decreased heat release rate of the composites. Graphene significantly decreases the mass loss rate of the composites, while the polymer contributes to a lower net enthalpy change of the composites because of its relatively lower individual enthalpy change.

4. Conclusions

The effect of graphene on the thermal stability and decomposition of polyimide was investigated. It was observed that the initial stage of degradation of polyimide follows the same pathway in both nitrogen and oxygen and this is not affected by the presence of graphene. Graphene was shown to lower the rate of mass loss of the composites by up to 198% at PI-50 wt.% graphene as it acts as a heat shield, protecting the underlying polymer matrix from external heat flux. It was also shown that the enthalpy of degradation of the polymer matrix was remarkably decreased by up to 1164% at 50 wt.% graphene.

The theoretical heat release rates were calculated from DSC thermograms. Results indicate that the heat release rate initially decreases by 62%, followed by a gradual increase as the graphene content in the composites increases. This was attributed to the higher heat of the combustion of graphene. Graphene lowers the rate of degradation of the polymer matrix, hence, the observed initial decrease in the heat release rate. However, increasing the graphene content also increases the heat of combustion of the composite, negating the effect of the reduced mass loss rate and leading to an overall increase in heat release rate. The onset temperature of degradation is observed to remain constant as the graphene content in the composites increases, hence, the ignitability of the polymer is presumed to remain unaffected by the presence of the graphene.

Author Contributions: Conceptualization, J.O.I. and C.J.A.; methodology, J.O.I. and C.J.A.; validation, C.J.A.; formal analysis, C.J.A.; investigation, C.J.A.; resources, J.O.I.; data curation, C.J.A.; writing—original draft preparation, C.J.A.; writing—review and editing, J.O.I. and C.J.A.; visualization, C.J.A.; supervision, J.O.I.; project administration, J.O.I. All authors have read and agreed to the published version of the manuscript.

Funding: This research received no external funding.

Institutional Review Board Statement: Not applicable.

Informed Consent Statement: Not applicable.

Data Availability Statement: The data presented in this study are available in within the article.

Conflicts of Interest: The authors declare no conflict of interest.

References

1. Gilman, J.W.; Harris, R.H.; Shields, J.R.; Kashiwagi, T.; Morgan, A.B. A study of the flammability reduction mechanism of polystyrene-layered silicate nanocomposite: Layered silicate reinforced carbonaceous char. *Polym. Adv. Technol.* **2006**, *17*, 263–271. [[CrossRef](#)]
2. Bartholmal, M.; Schartel, B. Layered silicate polymer nanocomposites: New approach or illusion for fire retardancy? Investigations of the potentials and the tasks using a model system. *Polym. Adv. Technol.* **2004**, *15*, 355–364. [[CrossRef](#)]
3. Morgan, A.B. The Future of Flame Retardant Polymers—Unmet Needs and Likely New Approaches. *Polym. Rev.* **2019**, *59*, 25–54. [[CrossRef](#)]
4. Morgan, A.B.; Harris, R.H.; Kashiwagi, T.; Chyall, L.J.; Gilman, J.W. Flammability of polystyrene layered silicate (clay) nanocomposites: Carbonaceous char formation. *Fire Mater.* **2002**, *26*, 247–253. [[CrossRef](#)]
5. Pack, S.; Si, M.; Koo, J.; Sokolov, J.C.; Koga, T.; Kashiwagi, T.; Rafailovich, M.H. Mode-of-action of self-extinguishing polymer blends containing organoclays. *Polym. Degrad. Stab.* **2009**, *94*, 306–326. [[CrossRef](#)]
6. Liu, M.; Zhang, X.; Zammarano, M.; Gilman, J.W.; Davis, R.D.; Kashiwagi, T. Effect of montmorillonite dispersion on flammability properties of poly(styrene-co-acrylonitrile) nanocomposites. *Polymer* **2011**, *52*, 3092–3103. [[CrossRef](#)]
7. Kashiwagi, T.; Harris, R.H.; Zhang, X.; Briber, R.; Cipriano, B.H.; Raghavan, S.R.; Awad, W.H.; Shields, J.R. Flame retardant mechanism of polyamide 6–clay nanocomposites. *Polymer* **2004**, *45*, 881–891. [[CrossRef](#)]
8. Manias, E.; Touny, A.; Wu, L.; Strawhecker, K.; Lu, A.B.; Chung, T.C. Polypropylene/Montmorillonite Nanocomposites. Review of the Synthetic Routes and Materials Properties. *Chem. Mater.* **2001**, *13*, 3516–3523. [[CrossRef](#)]

9. Strawhecker, K.E.; Manias, E. Structure and Properties of Poly(vinyl alcohol)/Na+Montmorillonite Nanocomposites. *Chem. Mater.* **2000**, *12*, 2943–2949. [[CrossRef](#)]
10. Cai, D.; Song, M. Recent advance in functionalized graphene/polymer nanocomposites. *J. Mater. Chem.* **2010**, *20*, 7906–7915. [[CrossRef](#)]
11. Gilman, J. Flammability and thermal stability studies of polymer layered-silicate (clay) nanocomposites. *Appl. Clay Sci.* **1999**, *15*, 31–49. [[CrossRef](#)]
12. Pradhan, B.; Setyowati, K.; Liu, H.; Waldeck, D.H.; Chen, J. Carbon Nanotube–Polymer Nanocomposite Infrared Sensor. *Nano Lett.* **2008**, *8*, 1142–1146. [[CrossRef](#)] [[PubMed](#)]
13. Calizo, I.; Balandin, A.A.; Bao, W.; Miao, F.; Lau, C.N. Temperature Dependence of the Raman Spectra of Graphene and Graphene Multilayers. *Nano Lett.* **2007**, *7*, 2645–2649. [[CrossRef](#)] [[PubMed](#)]
14. Lee, C.; Wei, X.; Kysar, J.W.; Hone, J. Measurement of the elastic properties and intrinsic strength of monolayer gra-phene. *Science* **2008**, *321*, 385–388. [[CrossRef](#)] [[PubMed](#)]
15. Balandin, A.A.; Ghosh, S.; Bao, W.; Calizo, I.; Teweldebrhan, D.; Miao, F.; Lau, C.N. Superior Thermal Conductivity of Single-Layer Graphene. *Nano Lett.* **2008**, *8*, 902–907. [[CrossRef](#)]
16. Du, X.; Skachko, I.; Barker, A.; Andrei, E.Y. Approaching ballistic transport in suspended grapheme. *Nat. Nanotechnol.* **2008**, *3*, 491–495. [[CrossRef](#)]
17. Bunch, J.S.; Verbridge, S.S.; Alden, J.S.; van der Zande, A.M.; Parpia, J.M.; Craighead, H.G.; McEuen, P.L. Impermeable Atomic Membranes from Graphene Sheets. *Nano Lett.* **2008**, *8*, 2458–2462. [[CrossRef](#)]
18. Morgan, A.B.; Putthanasarat, S. Use of inorganic materials to enhance thermal stability and flammability behavior of a polyimide. *Polym. Degrad. Stab.* **2011**, *96*, 23–32. [[CrossRef](#)]
19. Tandon, G.; Pochiraju, K.; Schoeppner, G. Thermo-oxidative behavior of high-temperature PMR-15 resin and composites. *Mater. Sci. Eng. A* **2008**, *498*, 150–161. [[CrossRef](#)]
20. Putthanasarat, S.; Tandon, G.P.; Schoeppner, G.A. Influence of aging temperature, time, and environment on ther-mo-oxidative behavior of PMR-15: Nanomechanical characterization. *J. Mater. Sci.* **2008**, *43*, 6714–6723. [[CrossRef](#)]
21. Pochiraju, K.V.; Tandon, G.P.; Schoeppner, G.A. Evolution of stress and deformations in high-temperature polymer matrix composites during thermo-oxidative aging. *Mech. Time Depend. Mater.* **2007**, *12*, 45–68. [[CrossRef](#)]
22. Lu, Y.C.; Tandon, G.P.; Jones, D.C.; Schoeppner, G.A. Elastic and viscoelastic characterization of thermally-oxidized polymer resin using nanoindentation. *Mech. Time Depend. Mater.* **2009**, *13*, 245–260. [[CrossRef](#)]
23. Ghosh, A.; Subrahmanyam, K.S.; Krishna, K.S.; Datta, S.; Govindaraj, A.; Pati, S.K.; Rao, C.N.R. Uptake of H₂ and CO₂ by Graphene. *J. Phys. Chem. C* **2008**, *112*, 15704–15707. [[CrossRef](#)]
24. Fornes, T.; Yoon, P.; Hunter, D.; Keskkula, H.; Paul, D. Effect of organoclay structure on nylon 6 nanocomposite morphology and properties. *Polymer* **2002**, *43*, 5915–5933. [[CrossRef](#)]
25. Cullis, C. The role of pyrolysis in polymer combustion and flame retardance. *J. Anal. Appl. Pyrolysis* **1987**, *11*, 451–463. [[CrossRef](#)]
26. Lua, A.C.; Su, J. Isothermal and non-isothermal pyrolysis kinetics of Kapton®polyimide. *Polym. Degrad. Stab.* **2006**, *91*, 144–153. [[CrossRef](#)]
27. Hatori, H.; Yamada, Y.; Shiraishi, M.; Yoshihara, M.; Kimura, T. The mechanism of polyimide pyrolysis in the early stage. *Carbon* **1996**, *34*, 201–208. [[CrossRef](#)]
28. Cella, J.A. Degradation and stability of polyimides. *Polym. Degrad. Stab.* **1992**, *36*, 99–110. [[CrossRef](#)]
29. Bürger, A.; Fitzer, E.; Heym, M.; Terwiesch, B. Polyimides as precursors for artificial carbon. *Carbon* **1975**, *13*, 149–157. [[CrossRef](#)]
30. Akinyi, C.; Longun, J.; Chen, S.; Iroh, J.O. Decomposition and Flammability of Polyimide Graphene Composites. *Minerals* **2021**, *11*, 168. [[CrossRef](#)]
31. Arnold, C.; Borgman, L.K. Chemistry and Kinetics of Polyimide Degradation. *Ind. Eng. Chem. Product Res. Dev.* **1972**, *11*, 322–325. [[CrossRef](#)]
32. Wunderlich, B. The heat capacity of polymers. *Thermochim. Acta* **1997**, *300*, 43–65. [[CrossRef](#)]
33. Yuan, B.; Sheng, H.; Mu, X.; Song, L.; Tai, Q.; Shi, Y.; Liew, K.M.; Hu, Y. Enhanced flame retardancy of polypropylene by melamine-modified graphene oxide. *J. Mater. Sci.* **2015**, *50*, 5389–5401. [[CrossRef](#)]
34. Song, Y.; Yu, J.; Yu, L.; Alam, F.E.; Dai, W.; Li, C.; Jiang, N. Enhancing the thermal, electrical, and mechanical properties of silicone rubber by addition of graphene nanoplatelets. *Mater. Des.* **2015**, *88*, 950–957. [[CrossRef](#)]
35. Pramoda, K.P.; Chung, T.S.; Liu, S.L.; Oikawa, H.; Yamaguchi, A. Characterization and thermal degradation of polyimide and polyamide liquid crystalline polymers. *Polym. Degrad. Stab.* **2000**, *67*, 365–374. [[CrossRef](#)]
36. Price, A.R.H.D. Combustion processes of textile fibres. In *Handbook of Fire Resistant Textiles*; Kilinc, F.S., Ed.; Woodhead Publishing: Cambridge, UK, 2013; pp. 3–25.
37. Biteau, H.; Steinhaus, T.; Schemel, C.; Simeoni, A.; Marlair, G.; Bal, N.; Torero, J. Calculation Methods for the Heat Release Rate of Materials of Unknown Composition. *Fire Saf. Sci.* **2008**, *9*, 1165–1176. [[CrossRef](#)]
38. Walters, R.N.; Hackett, S.M.; Lyon, R.E. Heats of combustion of high temperature polymers. *Fire Mater.* **2000**, *24*, 245–252. [[CrossRef](#)]
39. Jessup, R.S. Heats of combustion of diamond and of graphite. *J. Res. Natl. Inst. Stand. Technol.* **1938**, *21*, 475. [[CrossRef](#)]